Tectonics

Supporting Information for

Crustal and mantle deformation inherited from obduction of the Semail ophiolite (Oman) and continental collision (Zagros)

S. Pilia[1], A. Kaviani[2], M. P. Searle[3], P. Arroucau[4], M. Y. Ali[5], and A. B. Watts[3]

[1]Department of Earth Sciences-Bullard Labs, University of Cambridge, Cambridge, UK.

[2]Institute of Geosciences, Goethe University Frankfurt, Frankfurt, Germany.

[3]Department of Earth Sciences, University of Oxford, Oxford, UK.

[4]Electricité de France, Direction Industrielle, TEGG, Aix-en-Provence, France.

[5]Department of Earth Sciences, Khalifa University of Science and Technology, Abu Dhabi, UAE.

Contents of this file

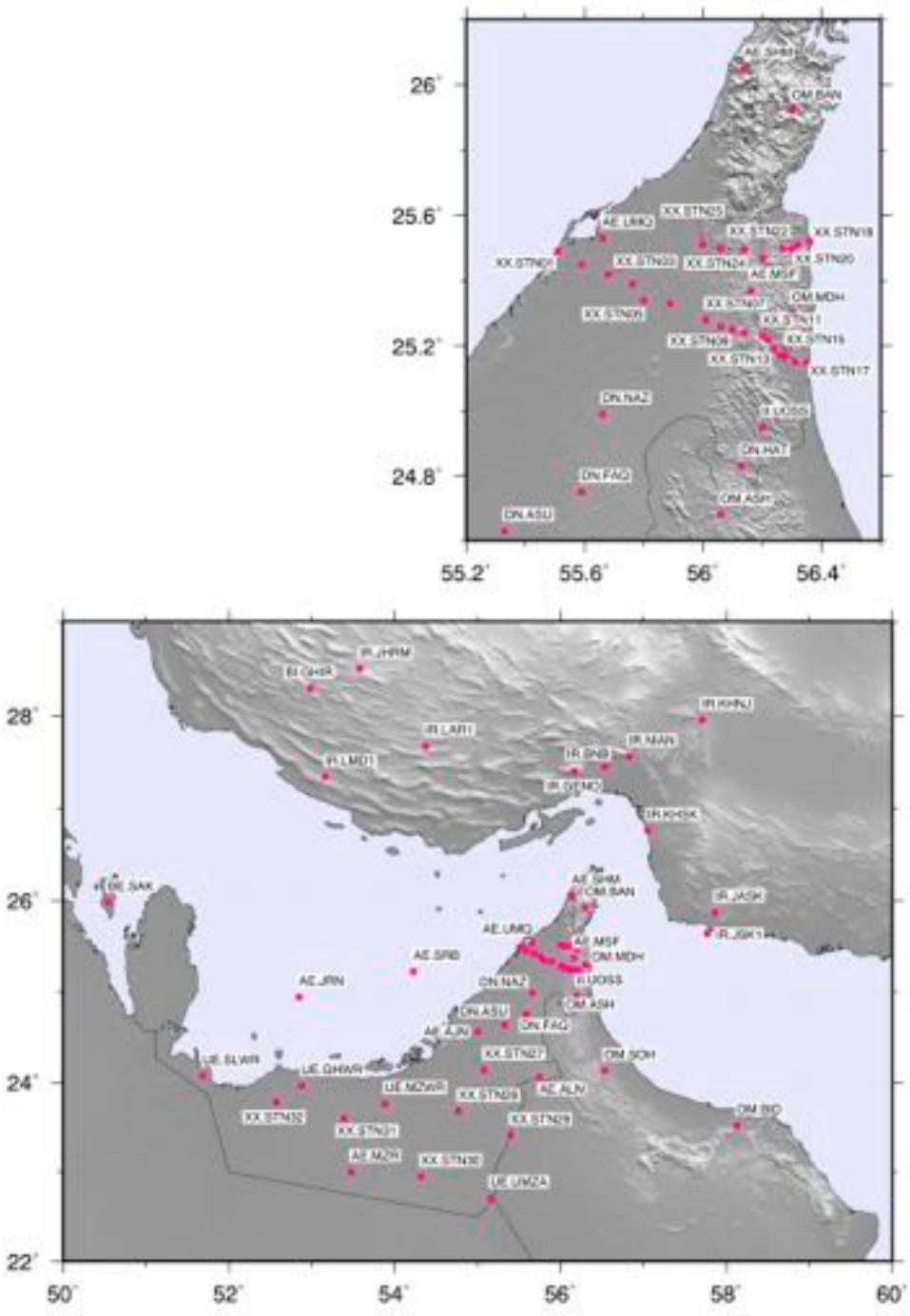

Figure S1. Location of all seismic stations used in this study with a zoom-in on the two transects across the Semail ophiolite. Station names are also included.

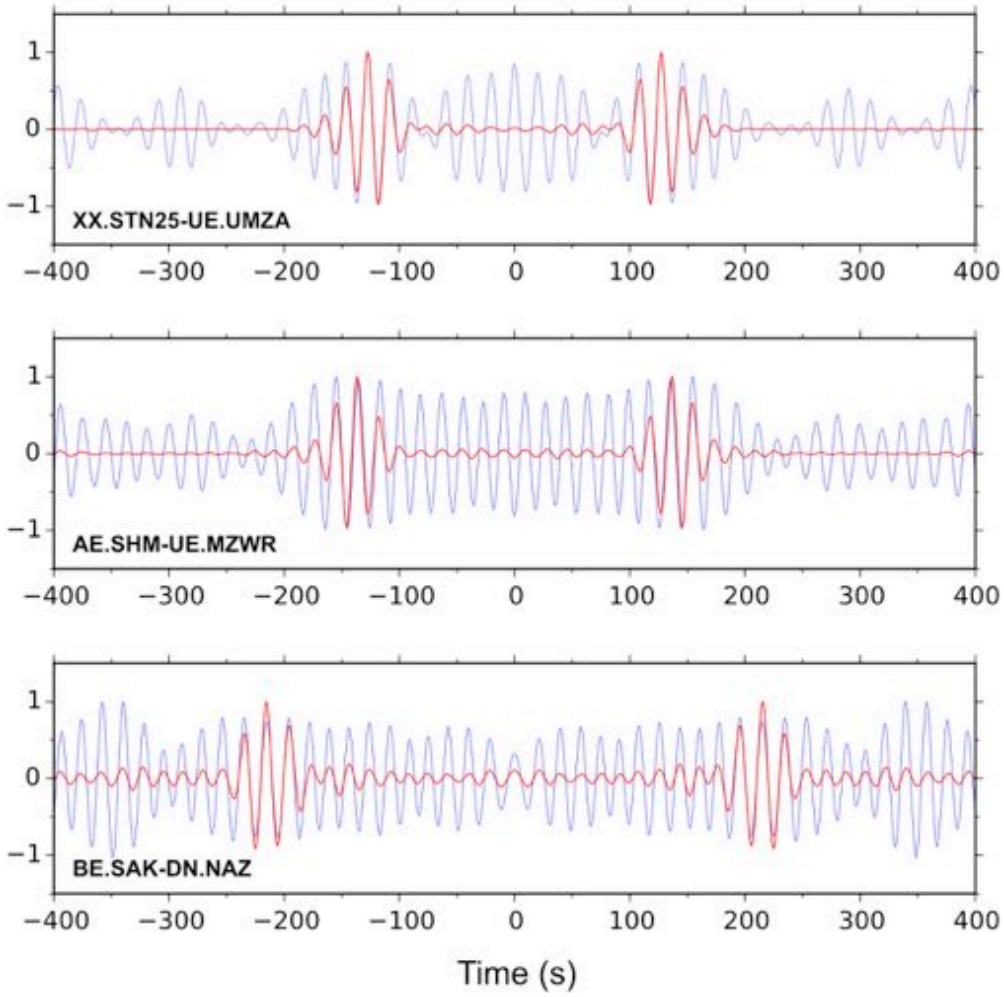

Figure S2: Three examples of symmetric cross-correlations obtained through the application of a conventional, amplitude-based stacking method (blue) and a non-linear method (red). Employment of the time-domain phase-weighted stacking procedure distinctly reduce the incoherent noise, which allows for better signal identification and subsequent phase velocity extraction. Amplitude has been normalized in all cases. For stations locations see Figure S1.

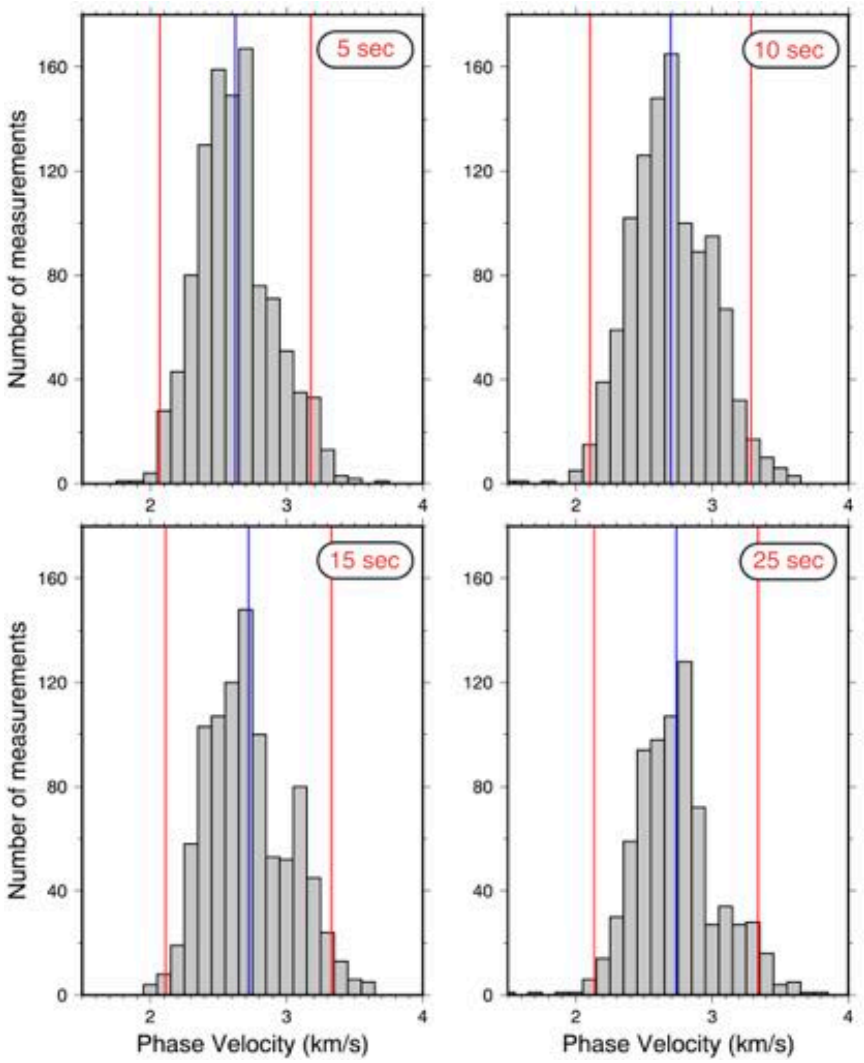

Figure S3: Histograms show dispersion measurements for all pairs of stations. Blue lines indicate the mean values and the red lines standard deviations. Only measurements within these 2 standard deviation thresholds are retained for the tomographic inversions.

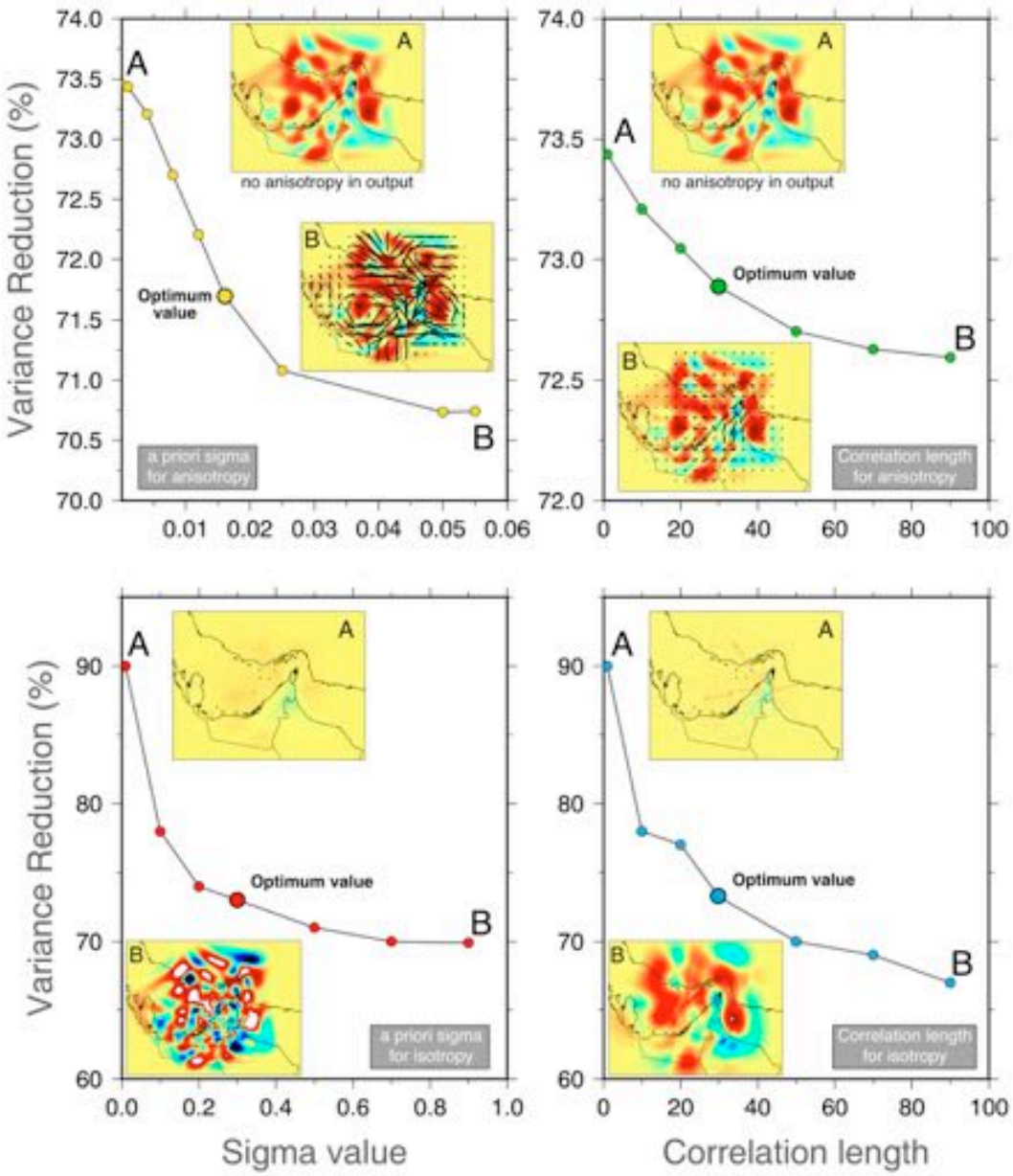

Figure S4: Example of trade-off curves used to determine the best values for isotropic and anisotropic L_{corr} and σ at 10 seconds. Although the tomographic algorithm allows us to use different correlation lengths for isotropic and anisotropic components of the wavefield, a value equal to 30 was found to be optimal for both.

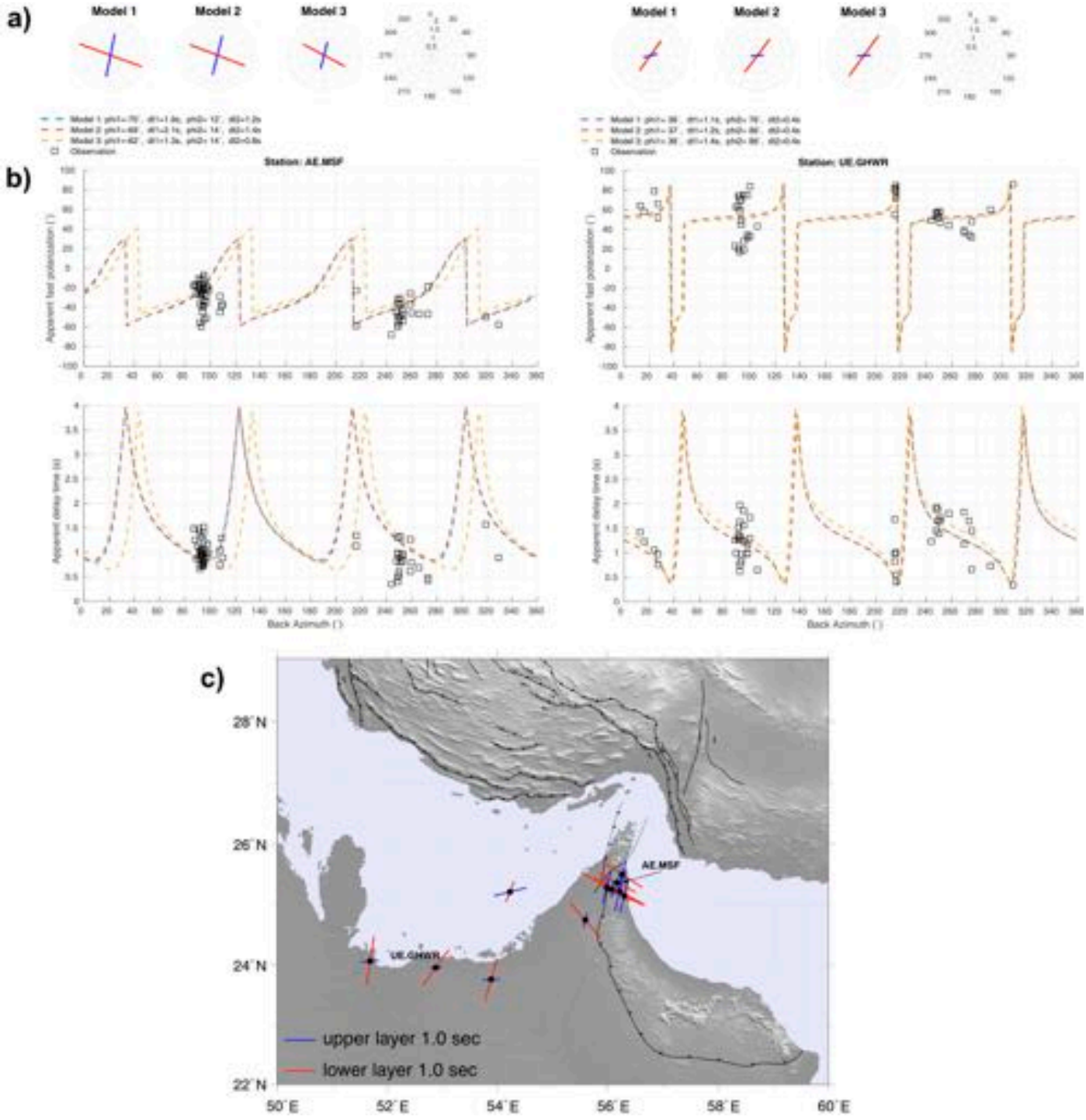

Figure S5: Two-layer modelling results. The direction of the upper-layer anisotropy is constrained to vary only around a direction defined by crustal anisotropy. a) shows two examples of two-layer modelling, computed for station AE.MSF (located in the UAE-Oman mountain range) and station UE.GHWR (located in southwest UAE). The parameters of the upper (blue lines) and lower layers (red lines) for three best models are shown for each station. b) shows the azimuthal variation of the observed splitting parameters (black squares) as well as the theoretical curves (dashed lines) for the best three models. Map in c) presents the two-layer models obtained at the stations where azimuthal coverage allows to study two-layer anisotropy.

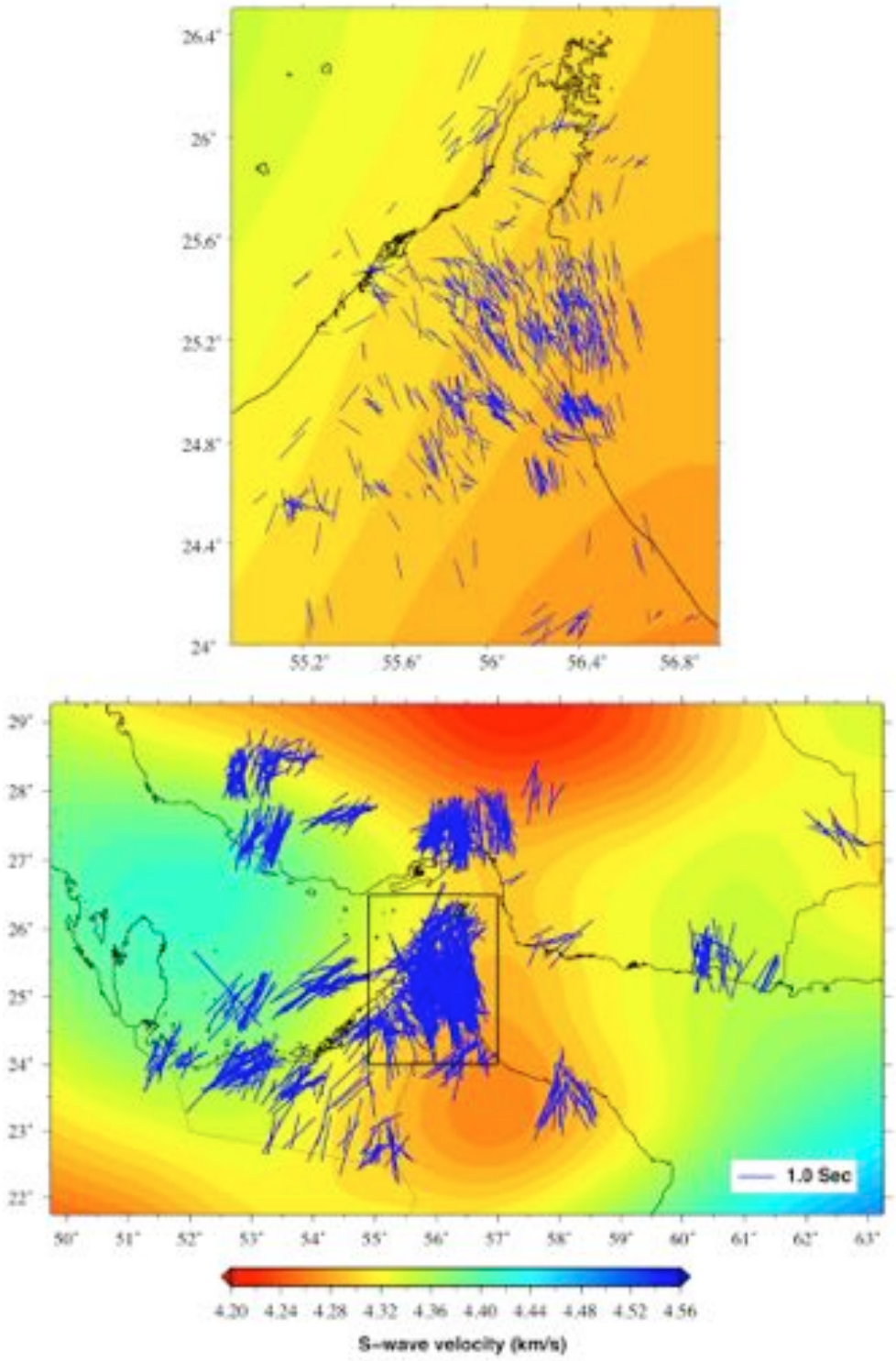

Figure S6: Ensemble of individual splitting parameters at 75 km depth for every station. Upper panel is a zoom-in on the two transects across the Musandam Peninsula. Background colors represent S-wave velocities from Priestley and McKenzie (2013).

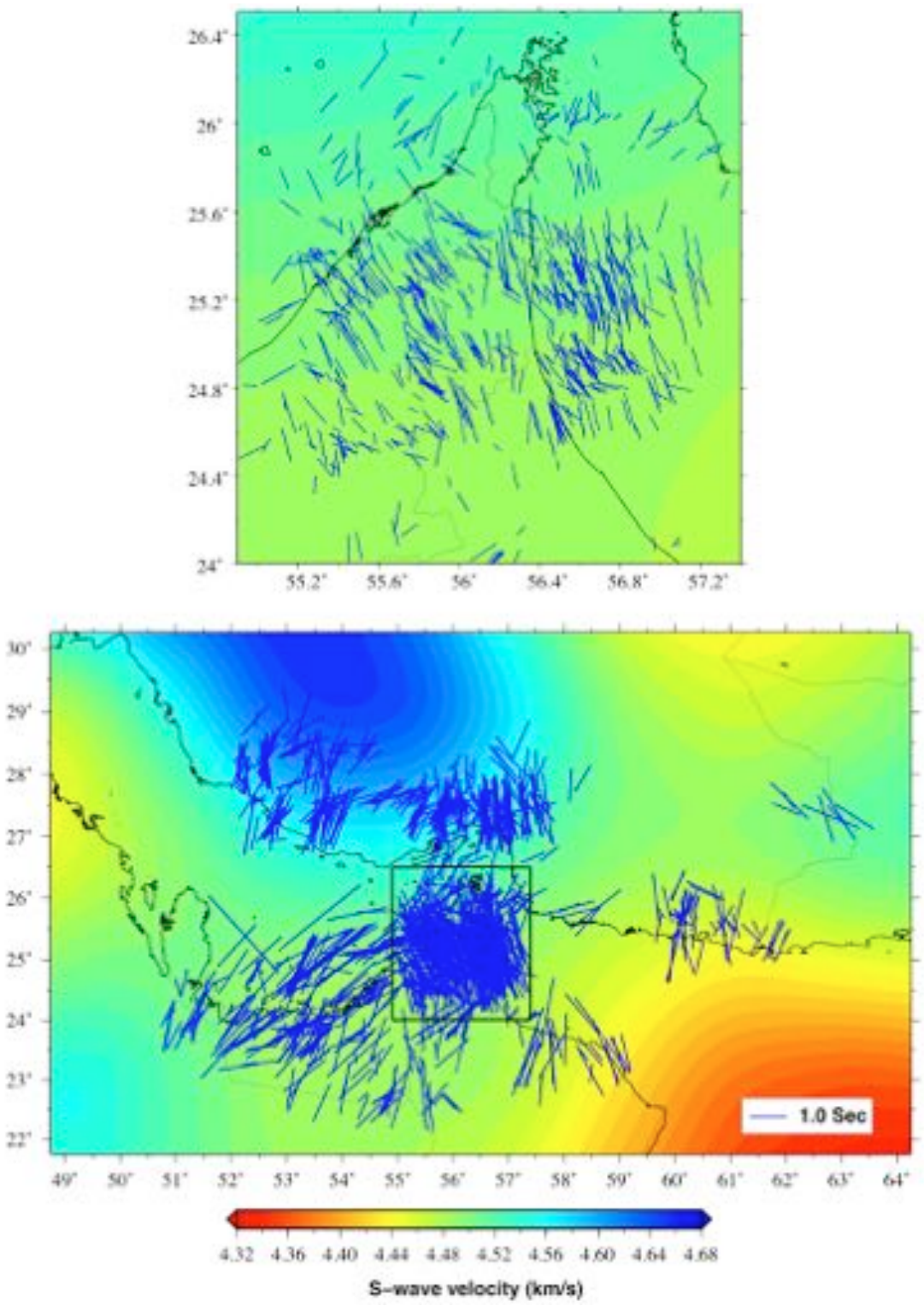

Figure S7: Ensemble of individual splitting parameters at 170 km depth for every station. Upper panel is a zoom-in on the two transects across the Musandam Peninsula. Background colors represent S-wave velocities from Priestley and McKenzie (2013).

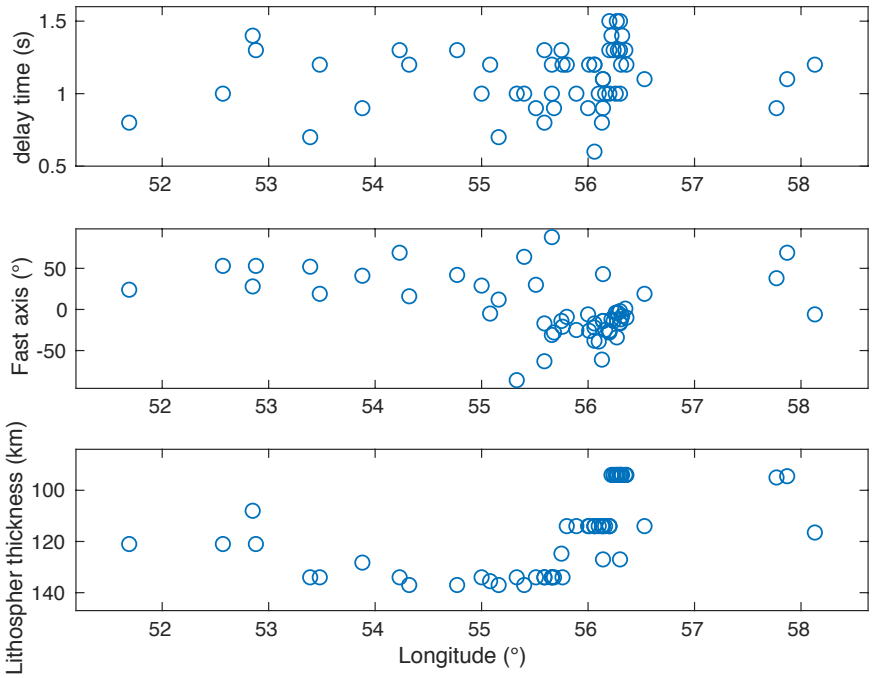

Figure S8: Plots of splitting parameters and lithospheric thickness as a function of longitude. A significant change in delay time with increasing lithospheric thickness is not observed.